Surface and thermodynamic interatomic force fields for silicon clusters and bulk phases

James R. Chelikowsky
Department of Chemical Engineering and Materials Science and Minnesota Supercomputer Institute, University of Minnesota, Minneapolis, Minnesota 55455

J. C. Phillips
AT&T Bell Laboratories, Murray Hill, New Jersey 07974-2070
(Received 30 October 1989)

We have developed new interatomic force fields which describe the phase stability of crystalline silicon and small clusters of silicon. We show that when three-body forces are adjusted to describe "covalent→metallic" phase transitions instead of small-amplitude atomic vibrations, a simple and accurate force field is obtained. This force field can be easily modified to describe energies and structures of Si_n vapor-phase clusters. A key aspect of the cluster problem is the transfer of bond strength from dangling bonds to back bonds. We expect our potential will have widespread applications to the formation and activation energies for diffusion of defects in crystalline Si and to the structural properties of amorphous and liquid silicon.

I. INTRODUCTION

The determination of the structure of extended nonperiodic systems such as clusters, liquids, and amorphous solids is one of the difficult problems in condensed-matter physics. For these systems, experimental probes cannot yield complete structural information. Probes for surface structure now exist, e.g., the scanning tunneling microscope, but not for bulk nonperiodic structures or clusters. Current *ab initio* quantum-mechanical methods have proved to be very useful for predicting the structure of small clusters. However, they are still too cumbersome to handle systems of sufficient size to make useful predictions for amorphous solids or liquids.

It would seem that for large numbers of atoms it should be possible to replace the complete quantum-mechanical description by a simpler classical interatomic-force-field model. Calculations with such a model can be carried out several orders of magnitude more rapidly than is possible with *ab initio* methods. However, at the atomic level our understanding of the quantum-mechanical forces is still in its infancy. While we easily understand the tetrahedral coordination of crystalline Si in terms of hybridized sp^3 orbitals, how can a classical model describe the metallic high-pressure phases of Si, or the Jahn-Teller reconstructions of Si surfaces? Indeed, what can we reasonably expect from classical forces? These questions have recently attracted much interest and have been answered in several ways. Here we present a new approach. We make detailed comparisons of our results both with the best available first-principles calculations and with the results obtained with other classical models. We believe that the present classical method is the only one which has yielded accurate results for both the bulk-phase diagram and cluster structural trends.

Before the coming of effective methods to compute the total energy of solids, one had to rely exclusively on an experimental data base of elastic constants and vibrational spectra for silicon in the diamond structure. However, this limited data base has changed dramatically in the last several years. Particularly, the theoretical work of Yin and Cohen on the high-pressure phases of silicon[1] has allowed one to have access to accurate information on more general configurations of crystalline silicon. Also, highly sophisticated molecular-orbital calculations[2] exist on Si_n for $n \leq 10$. On the experimental side, measurements on the vapor phases of Si_n^+ and Ge_n^+ clusters have been reported[3] for $2 \leq n \lesssim 60$. These developments have produced a new battery of data on silicon which encompasses the range from small clusters to many crystalline phases.

The process of transcribing quantum-mechanical forces into classical ones is not automatic or routine. It will no doubt be based on intuition instead of an analytic process. Also, considering that quantum forces are nonlinear and nonlocal, we might expect some "nonintuitive" classical forces, e.g., larger three-body terms than two-body terms.

Several attempts have been made to model the new data bases.[4-12] However, these models have met with only limited success. For example, when emphasis was placed on bulk phases, the resulting morphology for clusters was not consistent with the quantum-chemistry results. Conversely, when emphasis was placed on fitting structural information for silicon clusters, equations of state for the resulting bulk phases were poorly reproduced. These contradictions are easily understood. If "overcoordinated" silicon structures are fitted by classical potentials, there is no reason to suppose that "undercoordinated" cluster structures will be accurately reproduced, and vice versa. Most of the early work in this area concentrated in fitting bulk silicon polytypes such as the high-pressure phases, e.g., fcc and hcp structures. A

 ©1990 The American Physical Society

fit to such structures may reproduce twelvefold-coordinated silicon, but not twofold-coordinated silicon structures. Generally, when a particular data base is fitted, the resulting classical forces seldom prove accurate for regimes not included in the fit.

To ensure that our model has physical content, we demand that it provide accurate descriptions of two extreme systems: small clusters and various crystalline phases. Clusters contain many dangling bonds. We expect large reconstruction energies in the clusters owing to incomplete coordination.[2] Such reconstructions will be absent in the crystalline systems. These systems primarily are high-pressure phases where silicon is overcoordinated.[1] By incorporating both limits in our force-field description, we hope to enhance our capacity to describe systems which reside between these regimes. These intermediate cases would include structural defects, liquids, and amorphous solids.

II. CRYSTALLINE PHASES OF SILICON: THERMODYNAMIC INTERATOMIC FORCE FIELD

A. Defining a bulk-phase force field

Bond-stretching and bond-bending classical force fields (CFF) usually depend on the interatomic vector, $\mathbf{R}_{ij}$, between atoms i and j. These interactions are, respectively, functions of the magnitude of this vector and the dot product $\mathbf{R}_{ij}\cdot\mathbf{R}_{jk}$. A term involving $\cos(\theta_{ijk})$ commonly appears, where θ_{ijk} is the angle between $\mathbf{R}_{ij}$ and $\mathbf{R}_{jk}$. The key difference between our approach and that of previous CFF's is that we choose our angular function in a physical, rather than a geometrical way. Our function is designed to simulate the free-energy change at a metal-semiconductor transition. This transition is expected to be first order. The discontinuous transition involves large changes in the coordination and the conductivity of the silicon phases. For example, a relevant transition may involve converting the open, covalent fourfold-coordinated diamond structure to a metallic, compact, twelvefold-coordinated face-centered-cubic structure. An energy function which is discontinuous in a macroscopic sense is "S shaped" on an atomic scale.[13] The smallest bonding angle θ_{ijk} in the phases we consider varies from $\pi/3$ in a close-packed structure to $2\pi/3$ in graphite. If we use $\cos\theta_{ijk}$ to describe angular forces,[4-12] we are using a function which is nearly linear in the range of interest. However, if we instead use $\cos(3\theta_{ijk})$, then this function varies rapidly near $\theta_{ijk}=\pi/2$, corresponding to the metal-semiconductor transition, and slowly near $\theta_{ijk}=\pi/3$ (metallic phases) or near $\theta_{ijk}=2\pi/3$ (semiconducting phases).

While there are obvious advantages to using the physically significant function $\cos(3\theta_{ijk})$ instead of the geometrical function $\cos\theta_{ijk}$, there are disadvantages as well.[13] The geometrical function is single valued, but $\cos(3\theta_{ijk})$ is multiple valued. Thus while $\cos(3\theta_{ijk})$ has the correct qualitative behavior when θ_{ijk} is the smallest bond angle, if we were to use this function for all bond angles, there would be substantial cancellation of bond-bending energies between bond pairs with larger and smaller bond angles. This unwanted cancellation can be avoided[13] by imposing an angular cutoff which effectively retains only bond-bending energies for smaller bond angles.

The angular cutoff effectively erases the long-range phase coherence which is characteristic of quantum-mechanical wave functions in favor of short-range interaction energies. Because we are using a classical force field, we feel that this is logically the only correct procedure. All other attempts[4-12] to model interatomic forces in Si have used $\cos\theta_{ijk}$ summed over all bond angles (small and large) without an angular cutoff. While on geometrical grounds this approach seems safe enough, as well shall see our quite different approach yields dramatic improvements in the fit to the bulk-phase diagram. We believe that the origin of this success lies primarily in the fact that our model incorporates the basic physics of the metal-semiconductor transition in an internally self-consistent way. We also believe that this is not possible with $\cos\theta_{ijk}$ because this geometrical factor does not recognize the quantum-mechanical content of the metal-semiconductor transition which occurs between small and large values of the smallest bond angle. Our view is supported by the failure of *many* workers who used $\cos\theta$ to achieve good fits to the bulk-phase diagram, in spite of the fact that all of them used at least as many (often more) adjustable parameters as we have used.

The explicit expression for our thermodynamic interatomic force fields (TIFF) in the crystalline state is

$$E[\{\mathbf{R}\}]=\frac{1}{2}\sum_{\substack{i,j\\(i\neq j)}}[A\exp(-\beta_1 R_{ij}^2)/R_{ij}^2-g_{ij}\exp(-\beta_2 R_{ij}^2)/R_{ij}]\ , \tag{1}$$

where R_{ij} is the interatomic distance between (i,j) and the many-body forces which are contained within the factor g_{ij}. We wish g_{ij} to be large for covalent systems with large bond angles resulting in a shorter bond length R_{ij}, as compared to metallic systems with small bond angles.

We define g_{ij} as

$$g_{ij}=g_0+g_1 S_{ij}S_{ji}\ , \tag{2}$$

where

$$S_{ij}=1+\langle\cos(3\theta_{ijk})\rangle\ ,$$

$$\langle f(\theta_{ijk})\rangle=[f]/[1]\ ,$$

$$[f(\theta_{ijk})]=\sum_{\substack{k\\(i\neq k\neq j)}} f(\theta_{ijk})\exp(-\lambda_1\theta_{ijk}^4)\exp(-\lambda_2 R_{ijk}^4)\ ,$$

with $R_{ijk}=(R_{ij}+R_{ik})/2$. This form for f represents a very-short-range function which has sharp angular and radial cutoffs. The parameters (λ_1,λ_2) are fixed to be

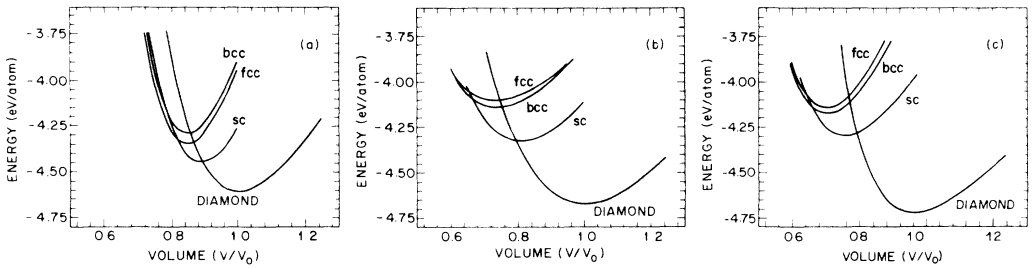

FIG. 1. Equation of state for silicon as a function of atomic volume. Shown are the body-centered-cubic (bcc), face-centered-cubic (fcc), simple-cubic (sc), and diamond structures. The volumes have been normalized to the experimental equilibrium volume of the diamond structure. We present results from (a) the interatomic potential of Biswas and Haman (Ref. 5), (b) the quantum-mechanical results of Yin and Cohen (Ref. 1), and (c) the present work.

$(\lambda_1)^{-1}=(\pi/2)^4$ and $(\lambda_2)^{-1}=R_0^4$, where R_0 is the nearest-neighbor distance in the diamond structure. The factor S_{ij} ranges from 0 for metallic systems to 2 for covalent systems. Also, for $\theta_{ijk}<\pi/3$ ($\theta_{ijk}>2\pi/3$) we saturate $\cos(3\theta_{ijk})$ so that $\cos(3\theta_{ijk})=-1$ (+1).

The parameters A, β_1, β_2, g_0, and g_1 are determined by fitting the equation of state at $T=0$ K for diamond, simple-cubic, body-centered-cubic, and face-centered-cubic Si structures as calculated by Yin and Cohen.[1] These structures have coordination numbers of 4, 6, 8, and 12, respectively. The equations of state for these structures can be accurately reproduced by the Murnaghan form:[14]

$$E(V)=\frac{B_0 V}{B_0'(B_0'-1)}\times\left\{B_0'\left[1-\frac{V_0}{V}\right]-\left[\left(\frac{V_0}{V}\right)^{B_0'}-1\right]\right\}+E(V_0). \tag{3}$$

This form requires knowing the equilibrium energy $E(V_0)$, volume V_0, bulk modulus B_0, and pressure derivative of the bulk modulus B_0'. The data base from Yin and Cohen provides roughly twice the number of points to be fitted as parameters. The resulting parameters for our interatomic potential are given in Table I.

B. Bulk phases of silicon

Our TIFF results for the equations of state are compared in Fig. 1 to Biswas and Hamann's CFF work[5] and to the Yin-Cohen quantum-mechanical calculations.[1] Our TIFF potential does a better job of replicating the quantum-mechanical results than does the CFF work. This is true even though the Biswas-Hamann potential requires more parameters, and is more successful in fitting the bulk-phase diagram than any of the other $\cos\theta$ models. Specifically, the equilibrium volume and placement of the bcc and fcc phases are reproduced better in

TABLE I. Parameters for the bulk terms of our interatomic potential for silicon. See Eqs. (1) and (2) and the text for details.

A (eV Å^2)=182.44	β_2 (Å^{-2})=0.151
β_1 (Å^{-2})=0.550	g_1 (eV Å)=2.644
g_0 (eV Å)=7.08	$\lambda_1=(2/\pi)^{-4}$
λ_2 (Å^{-4})=0.1773	

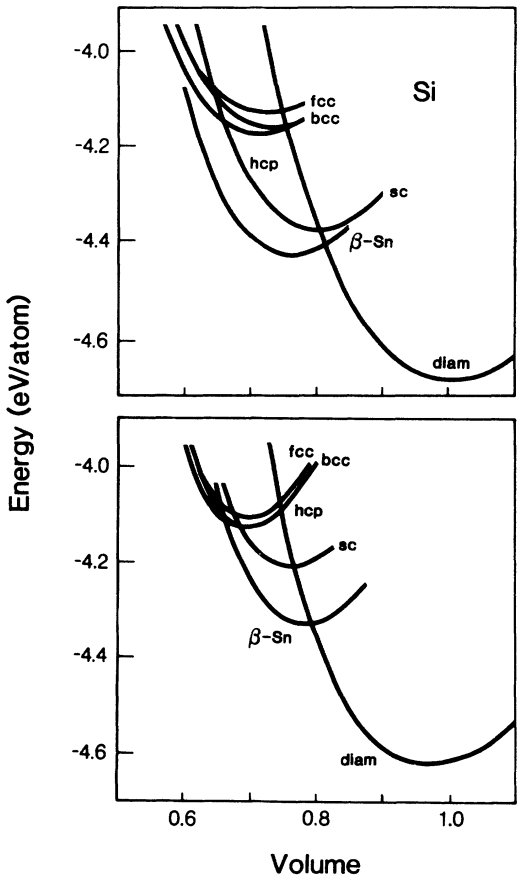

FIG. 2. Equation of state for silicon including the hexagonal-close-packed (hcp) and the white-tin structure (β-Sn). The top panel is from the work of Chang and Cohen (Ref. 15); the bottom panel is from our interatomic field.

TABLE II. Equation-of-state parameters for silicon in various structures. See Eq. (3). Sources of experimental and pseudopotential values discussed in text.

Structure	Cohesive energy (eV)	Lattice constants (Å)	Bulk modulus (Mbar)	Derivative of bulk modulus with pressure
Diamond				
Present work	4.62	5.36	1.01	5.00
Experiment	4.63	5.43	0.99	
Pseudopotential	4.84	5.45	0.98	
β-Sn	4.33	4.64(a) 2.89(c)	1.50	4.26
Simple-cubic	4.21	2.47	1.47	5.37
Hexagonal-close-packed	4.13	2.71(a) 4.41(c)	1.81	5.05
Body-centered-cubic	4.13	3.03	1.90	6.07
Face-centered-cubic	4.11	3.81	1.80	4.94

our work. We also obtain the correct ordering in energy of the bcc and fcc phases, although the energy difference between these phases is quite small.

In Fig. 2, we compare our work to the equations of state calculated by Chang and Cohen.[15] Their work is an extension of the work of Yin and Cohen.[1] In this figure, we have included two additional structures; the white-tin structure (β-Sn) and the hexagonal-close-packed (hcp) structure. We did not fit our potential parameters explicitly to either structure. Nonetheless, the agreement with Chang and Cohen is quite good. In Table II, we summarize the calculated equation-of-state data and compare to other theories and experiments. For the diamond structure, our calculated values for $B_0, E(V_0)$ and V_0 are comparable to the best theoretical values.

We find that the hcp structure is ~ 0.02 eV lower than the fcc structure and that its equation of state is almost identical to the bcc equation of state. Chang and Cohen find a similar placement for the hcp structure relative to the fcc structure. They found a c/a ratio of 1.69, which is larger than the ideal ratio, but is consistent with experimental values ranging from 1.64 to 1.70. Our potential yields an ideal c/a ratio of 1.63 to within $\sim 1\%$. Also, Chang and Cohen find a larger separation between bcc and hcp than we do. To within ~ 5 meV, we find the same equilibrium energy for the bcc and hcp structures. Our accuracy in the fitting is probably ~ 10 meV, so we cannot distinguish between bcc and hcp structures.

The β-Sn structure can be considered a "transition structure" from the covalent diamond structure to a metallic structure. The β-Sn coordination is rigorously fourfold, but the two next nearest neighbors are only $\sim 5\%$ more distant. Thus β-Sn can be considered to be sixfold coordinated, or a Jahn-Teller distorted octahedron. Our equilibrium volume for β-Sn is slightly larger than predicted by Chang and Cohen. Otherwise, the equations of state are similar. With respect to our c/a ratio, we find a value of about 0.62, as opposed to the quantum-mechanical prediction and experimental[16] value of 0.55. Our larger c/a ratio can be attributed to the angularly dependent energy factor in (2). A larger c/a ratio would produce larger angles θ_{ijk}, which are closer to the tetrahedral angle. Perhaps a slightly weaker angular dependence would improve the c/a values.

We have examined the stability of the diamond structure versus the β-Sn structure as a function of pressure. We find that at ~ 140 kbar the diamond structure will transform to the β-Sn structure. This value is higher than experiment,[16–19] which ranges from 88 to 125 kbar, and higher than the quantum-mechanical predictions. The value of the transition volume for the diamond and β-Sn structures is quite good. Given that we have not adjusted our parameters to the pressure data, the agreement is surprisingly good and very much better than would be obtained by other currently available interatomic potentials based on $\cos\theta$. In Table III, we summarize our pressure calculations and compare to experiment and other theories.

TABLE III. Transition pressures and volumes for the cubic diamond to β-Sn transition. The transition volumes (V_t) are normalized to the experimental equilibrium volume of the diamond structure (20.01 Å^3/atom). The pseudopotential work is from Chang and Cohen (Ref. 15). Experimental data are from (a) Jamieson (Ref. 17) and (b) Hu and Spain (Ref. 20).

		V_t (diam.)	V_t (β-Sn)	Pressure (kbar)
Present work		0.87	0.72	140
Pseudopotential		0.93	0.72	93
Experiment	(a)	0.918	0.710	126
	(b)	0.911	0.706	113

III. SILICON CLUSTERS: SURFACE INTERATOMIC FORCE FIELD

A. Dangling-bond corrections to the bulk force field

If we apply our TFF potentials to small silicon clusters, we find the lowest-energy structures to be rings for Si_n

where $n<8$. For $n\geq 8$, we find a three-dimensional structure where the rings are capped off. In Fig. 3, we illustrate the lowest-energy structures for $n\leq 10$. We note that for $n=10$ we obtain the adamantine cage. The adamantine cage can be considered to be a diamond-structure fragment. It is noteworthy that we obtain this fragment, as it strongly suggests that diamond is the true ground-state structure for our bulk-silicon potential. For structures larger than $n=10$, we continue to build up "bulklike" fragments of "diamondlike" silicon. In Fig. 4, we illustrate typical structures for $n=13$, 16, and 19. Si_{19} is interesting in that it resembles graphitic rings linked by fivefold-coordinated rings. Such structural units are expected for covalent networks.

Our results based on the bulk-silicon potential are at strong variance with the structures obtained from molecular-orbital theory. The quantum-chemistry study of silicon clusters by Raghavachari and Rohlfing[2] yields three-dimensional structures for $n>5$. Moreover, the average coordination of their structures may exceed 4 (especially for $n>6$), which is indicative of a metallic structure. The quantum-chemistry work is similar to that found by other theoretical methods.[21] In contrast, the average coordination of the clusters in Fig. 3 never exceeds 2.5.

This disagreement between the structures predicted from our bulk-phase potential and those predicted by quantum chemistry is not surprising. Structural features which are associated with undercoordinated atoms, i.e., dangling-bond features, are not described by our bulk energy. To remedy this omission, we must modify our potentials for undercoordinated species.

Specifically, the transfer of dangling-bond strength to backbonds can produce more compact or more metallic structures. This transfer will depend on the angle θ_{ij} between the dangling bond and backbond. Let us define a "dangling-bond vector", $\mathbf{D}$, as follows:

$$\mathbf{D}_i=\frac{-\sum_{\substack{j\\(j\neq i)}}\mathbf{R}_{ij}\exp(-\lambda_3 R_{ij}^4)}{\sum_{\substack{j\\(j\neq i)}}\exp(-\lambda_3 R_{ij}^4)}\ . \tag{4}$$

We expect that backbonding strengthening will vary with the angle θ_{ij}. For covalent systems where $\theta_{ij}\sim 2\pi/3$ we expect large reconstructions. For metallic systems where $\theta_{ij}\sim\pi/2$ we expect much less reconstruction. We describe the backbonding stengthening by the factor

$$Q_{ij}=1+zD_i\sin[\alpha(\theta_{ij}-\pi/3)]\ . \tag{5}$$

For metallic surfaces where $\theta_{ij}\approx\pi/2$, $Q_{ij}\approx 1$. For crystals,[5] $Q_{ij}=1$ as $D_i=|\mathbf{D}_i|$ is zero. D_i is small in clusters, except for surface atoms. By making clusters more compact, backbonding reduces covalent interactions and increases metallic interactions. To minimize the number of parameters, we assume that for each interaction ij,

$$\Delta g_0/g_0=-\Delta g_1/g_1=\mu(Q_{ij}Q_{ji}-1)\ . \tag{6}$$

The change in (g_0,g_1) vanishes for crystals. We need to determine four backbonding parameters: z, α, μ, and λ_3. We used the molecular-orbital studies of Raghavachari and Rohlfing[2] for structural properties and energies of Si_n clusters with $n\leq 10$ to fix our four parameters. The parameters are given in Table IV.

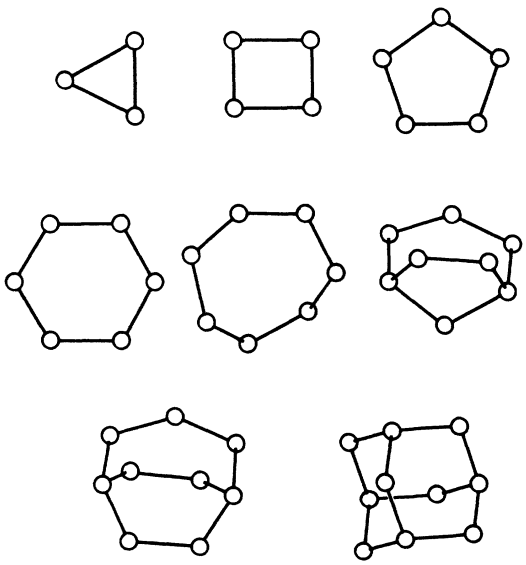

FIG. 3. The structure of Si_n with $3\leq n\leq 10$ without backbonding contributions. These structures disagree with those obtained from quantum-chemistry calculations[2] as the effect of dangling bonds are not included.

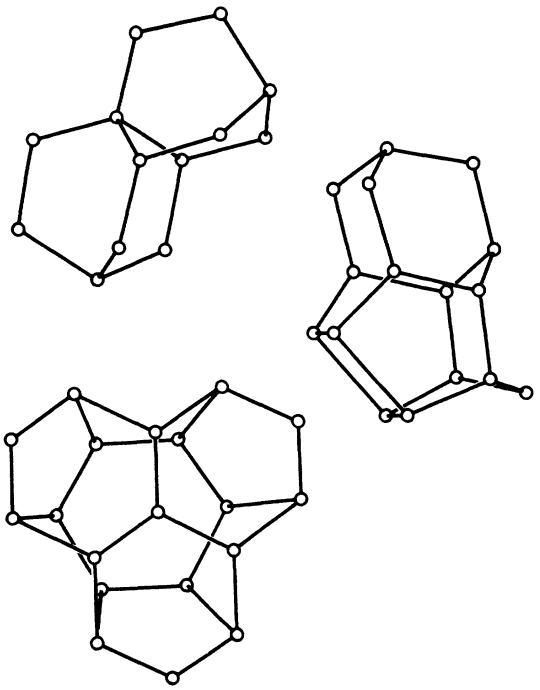

FIG. 4. Structures of Si_n for $n=13$, 16, and 19 without backbonding contributions. Note how these structures resemble fragments of the diamond structure.

TABLE IV. Parameters for the dangling-bond corrections to the bulk force field. See Eqs. (4)–(6) and the text for details.

λ_3 (Å^{-4})=0.023 79	z (Å^{-1})=0.0951
μ=4.0	α=1.70

One complication of this procedure is that the quantum-chemistry clusters may exhibit Jahn-Teller distortions. Especially for small clusters, these effects may be significant and will break symmetry. We expect the nature of the symmetry breaking to depend on valence-electron filling of specific molecular orbitals. Such effects cannot be included in our classical model. However, with increasing cluster size we expect that steric hindrance will reduce Jahn-Teller effects. The structures obtained from our potential should become much more reliable for $n > 10$.

B. Determining minimum-energy structures

For elemental crystalline matter, usually only a few lattice parameters are necessary to determine the structure. One can vary these lattice parameters to determine the lowest-energy structure. The problem is considerably more complex for clusters. For small clusters, it is possible to construct an inventory of structures and explore each topologically distinct case.[2] However, the number of possible structures grows so rapidly that this approach becomes impractical for more than about ten atoms.

There are several techniques to minimize a multiparameter function. We have used both a Monte Carlo (MC) simulated-annealing algorithm and a molecular-dynamics (MD) approach. In the MC method, we begin by randomly placing Si atoms in a cube. Each atom is required to be at least 3.5 Å from its neighbor and from the walls. The cube is heated initially to about 5000 K. We displace each atom in random discrete steps and determine the change in energy ΔE. If the energy of the cluster is lowered, then the step is accepted. If the energy is raised, the step is accepted with a probability given by $P=\exp(-\Delta E/kT)$. At high temperatures, steps which raise the energy are commonly accepted. As the temperature is lowered, eventually only steps which lower the energy are accepted. Provided the temperature is lowered slowly enough, and provided enough steps are taken, the resulting structure should be a global minimum in terms of the structural energy.

One method of determining the optimal step size is to adjust the step size to maintain a success rate of 50% in the steps taken.[22] We have used an alternative procedure which produces similar results, yet is somewhat easier to implement. We scale the step size so that the maximum step size $\delta R_{\max}$ is given by $\delta R_{\max}(T) = \delta R_{\max}(T_{\text{initial}})(T/T_{\text{initial}})^{1/2}$. This is the scaling one would expect in a Debye solid. As the cluster condenses into a stable state, one expects that a Taylor series of the energy would not contain terms linear in the atomic coordinates. In this regime, $\Delta E/kT \approx$ constant and $P \approx$ constant. An acceptance rate of 50% can be maintained as temperature is lowered through a judicious choice of $\delta R_{\max}(T_{\text{initial}})$, which we find is about 0.5 Å. Our annealing scheme employed 100 temperature divisions between T_{initial} and T_{final} (which was taken to be 100 K). The temperature anneal schedule is such that for the Nth division $T_N=\gamma T_{N-1}$ where $\gamma=0.96$. For each temperature division, we took 500 steps per particle. The total number of steps was 50 000 per particle with an anneal rate of about 10 MC steps/atom K. These parameters are similar to ones used in MC work on amorphous silicon.[22]

To see whether this annealing process is adequate, we performed two tests. First, we constructed an inventory of all the structures of Si_n examined in molecular-orbital calculations.[2] We then scaled the bond lengths in these structures until a minimum in the energy was achieved. This procedure resulted in an upper bound on the lowest-energy structure. Then we used our MC algorithm to determine the structure. If the MC method did not yield a structure with a lower energy, we then annealed more slowly until we obtained a lower-energy structure. As a second test we did some MD simulations.

To set up the MD program, we embedded our cluster in a viscous heat bath. Random initial velocities and coordinates were assigned to each atom. The equation of motion for the X component of the ith particle was given by

$$M\ddot{X}_j = -\partial E(\{\mathbf{R}_{ij}\})/\partial X_j - M\beta\dot{X}_j + G(T) , \tag{7}$$

where M is the mass of the atom, $E(\{\mathbf{R}_{ij}\})$ is given by Eqs. (1), (2), and (4)–(6), β is the viscosity parameter, and G is a randomly fluctuating force. Quite generally β and G are related by the fluctuation-dissipation theorem,[23] i.e., the probability of a random force G is given by $P(G)=(2\pi\sigma)^{-1/2}\exp(-G^2/2\sigma^2)$, where $\sigma=(2\beta MkTh^{-1})^{1/2}$, and h is the time step used to integrate (7). We use the numerical integration described by Tully *et al.*[23]

The MD approach to the structure was used to check the MC results. In the MD calculations, we started with a heat bath whose temperature was on the order of 3000 K. The temperature of the bath was slowly lowered to 100 K. The temperature anneal schedule is similar to that used for Monte Carlo runs, i.e., for the Nth division $T_N=\gamma T_{N-1}$, where $\gamma=0.9$. Approximately 30 temperature divisions were used with about 300 integration steps per division. The viscosity parameter was similar to that proposed by Wang and Chen.[24] Specifically, for our time step we take $h=300$ a.u. (1 a.u.$=2.42\times10^{-17}$ s) and for the viscosity $\beta=0.001$ a.u.$^{-1}$. Our total anneal time is $\sim$0.1 nsec. We did not repeat the MC work for each structure, but examined the Si_n clusters, with $n=10$, 13, 16, and 19. We are reasonably confident that the lowest-energy structures we present are global minimums. However, given the possibility of large kinetic barriers, one can never be "absolutely certain."

C. The structure of Si_n for $n \leq 20$

In Figs. 5 and 6 the minimum-energy structures for Si_n for $n \leq 20$ are illustrated. We find a much higher average coordination, unlike the structures with no backbonding

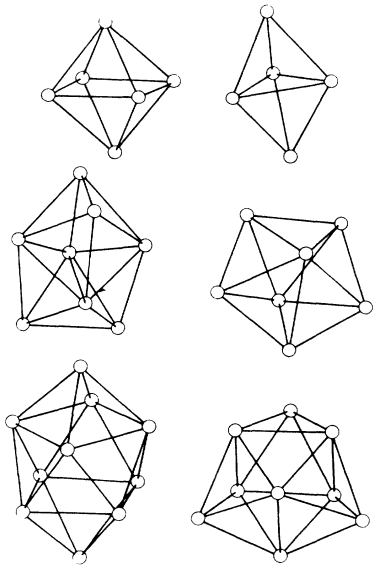

FIG. 5. The structure of Si_n with $4 \leq n \leq 10$ with backbonding contributions. These structures resemble with those obtained from quantum-chemistry calculations (Ref. 2) as the effect of dangling bonds is included.

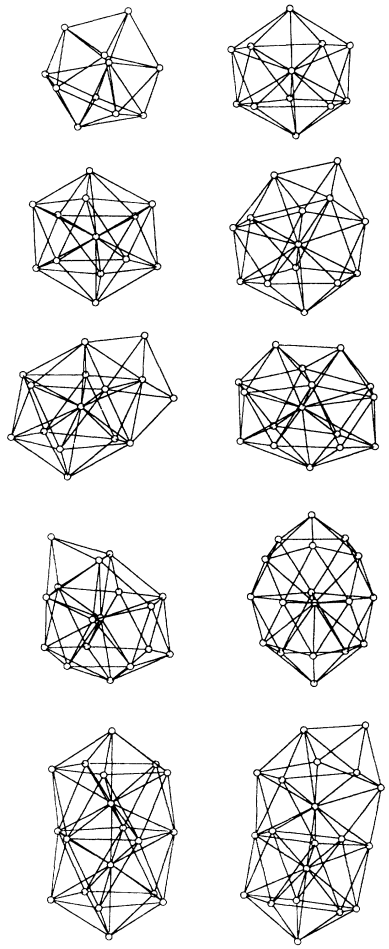

FIG. 6. The structure of Si_n with $11 \leq n \leq 20$ with backbonding contributions. Note how these structures are close packed in contrast to Fig. 4. The structure of these clusters is dominated by a pentagonal growth sequence.

corrections. This is expected with the increase in central-force interactions at the expense of angular interactions [see Eq. (6)]. In Fig. 7, we present a quantitative comparison of the average coordination for the clusters with and without backbonding. We define two atoms to be coordinated if the distance between atoms is less than a given distance R_0. Here we define R_0 to be 3 Å. [We have also defined coordination by a weighting function similar to that in Eq. (4) for $\mathbf{D}_i$. The results are quite similar.] We also compare to the quantum-chemistry work of Raghavachari and Rohlfing.[2] Clearly, the presence of a backbonding term results in a much improved agreement in compactness between the quantum-chemistry structures and those obtained from our interatomic potentials.

We obtain similarly coordinated structure as from the quantum-chemistry calculations for silicon clusters for $n \leq 10$; however, the structures often differ in detail. For example, $n = 8$ is a bicapped octahedron in both cases. Our interatomic potential yields a structure where adjacent faces are capped. For the quantum-chemistry work, opposite faces are capped.

For silicon clusters with $n > 10$, the geometries are very different than one what might have expected based on the bulk-phase diagram in Figs. 1 and 2. The dominant structural feature in Fig. 6 is the icosahedron. This is reflected in Fig. 7, where we have an anomalously large average coordination at $n = 13$ and $n = 19$. These structures correspond to ideal icosahedral structures. For example, the $n = 13$ structure is that of an atom-centered icosahedron. The $n = 13$ structure can be considered to be composed of 1-5-1-5-1 layers. This is the second element of a pentagonal growth sequence[25] which began with $n = 7$ (the bicapped pentagon with a 1-5-1 sequence).

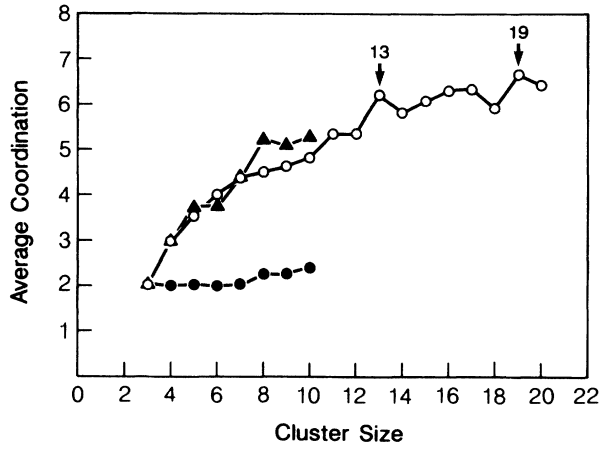

FIG. 7. The average coordination of Si_n. Shown are results from quantum-chemistry calculations[2] ($-\blacktriangle-\blacktriangle-$), and our interatomic force field ($-\bullet-\bullet-$) without backbonding corrections for Si_n with $n \leq 10$. Also shown are results for our interatomic potential ($-\circ-\circ-$) with backbonding corrections for $n \leq 20$. Note the anomalously high coordination for $n = 13$ and $n = 19$ which correspond to icosahedral structures.

The continuation of this sequence leads to the $n=19$ structure which is the double icosahedron, i.e., a 1-5-1-5-1-5-1 sequence. We have preliminary results which suggest that the sequence continues with a stable $n=25$ triple icosahedron.

Such metalliclike structures may seem surprising for silicon clusters. Icosahedral pentagonal growth sequence structures have occurred previously for two-body central-force potentials, e.g., metallic or inert-gas clusters. Magic numbers with $n=13,19,(23 \text{ or } 25),\ldots,55$, etc. have been observed for Xe and other inert-gas clusters.[26] However, our structures result from potentials which possess strong angular character, as evidenced by the bulk phases in Figs. 1 and 2. Our calculations show that backbonding forces in small clusters can cause a remarkable reappearance of these simple geometric structures.

Our model also shows for a wide range of parameters that at $n=11$, 12, 16, 17, and 18 these clusters do not belong to a simple pentagonal growth sequence. Instead we have a layered character similar to that of one of the $n=10$ isomers[2,21] which has a 3-3-3-1 trigonal prismatic structure. We find that $n=16$ corresponds to 1-6-1-6-2 and $n=17$ corresponds to capping off a face on the $n=16$ structure. For $n=18$, we have a 1-5-6-5-1 stacking sequence. It is tempting to suppose that the icosahedral structures are related to the closed-packed bulk phases, while the other uniaxial structures are related to the β-Sn bulk phase.

In Fig. 8, we present the cluster energies as a function of size and again compare the results to quantum-chemistry calculations. The absolute values of the cluster energies from quantum-chemistry calculations have been adjusted by rescaling of the correlation energy.[2] Owing to such difficulties in estimating the binding energies, we feel at this stage one should concentrate on the structural aspects. Nonetheless, the agreement is adequate, although some noticeable difference do occur. For example, the energy of Si_8 is lower per atom than the cluster energy of Si_7 in the quantum-chemistry calculation, whereas the opposite is observed in the interatomic potential work. Similar results have been observed using other interatomic potentials.[27] We also illustrate in Fig. 8 a liquid drop model curve fit to the interatomic potential. We used a simple expression of $E(n)/n = E_b(1-an^{-1/3}-bn^{-2/3})$ for this fit. If we fit (a,b) to our cluster energies for $n>6$, we obtain an estimate for the bulk binding energy E_b of about 4.9 eV/atom.[28] This value is remarkably close to the diamond-structure binding energy of 4.6 eV/atom.

From Fig. 8, we note that $n=6$, 10, 13, and 19 are especially stable. This stability has been confirmed by theory[2] and experiment[29] for $n=6$ and 10 ($n=7$ is also a stable cluster). For larger clusters, so far it has not been possible to determine which are most stable. Careful studies[30] of the effect of ionizing laser energy and intensity on beam distributions have revealed cluster-fragmentation effects which are likely to be strong for "metallic" clusters. Such an effect precludes inference of relative cluster energies from beam distribution intensities in cases where the ionization energies I_n are large (in Si_n $I_n>7$ eV for $n<10$).

In Fig. 9, we present the radial distribution functions averaged over the clusters for $n\leq 20$. We obtain a distinct separation between first and second neighbors which allows us to make a satisfactory definition of coordination numbers. It is interesting that the ratio of the nearest neighbor to the next-nearest neighbor for our clusters is similar to that of the diamond structure. In Fig. 10, we consider how the bond length varies with coordination. We find a somewhat complex behavior. For coordination numbers (CN) at CN of 4 and 12, we find much smaller bond lengths than at other coordinations, e.g., a maximum occurs at a CN of ~6–8. If we consider the bond strength to be related to a bond length, then we would expect strong bonds to be formed with CN of 4 or 12 and weak bonds with a CN of 6–8. Again, this would reflect our covalent (a CN of 4) to metallic transition (a CN of 12). Note that for a CN of 12, triangles of nearest neigh-

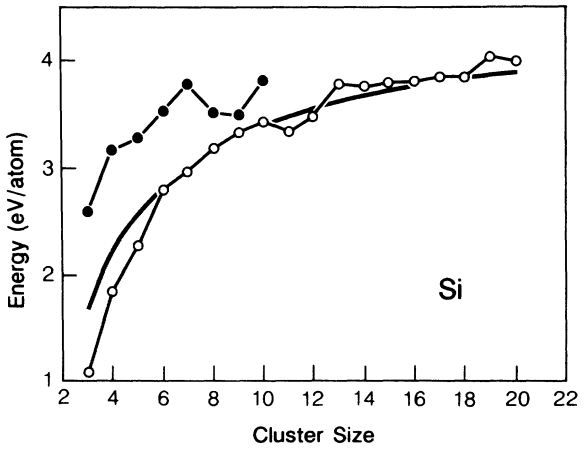

FIG. 8. The binding energy of Si_n. Shown are results from quantum-chemistry calculations (Ref. 2) (—●—●—), from our interatomic force field (—○—○—), and from the liquid drop model (—).

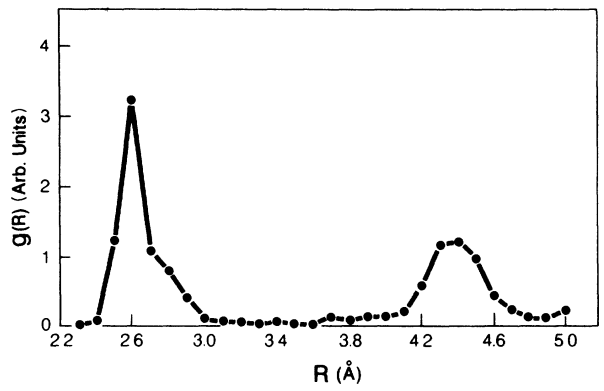

FIG. 9. Radial distribution function for Si_n averaged over $n\leq 20$.

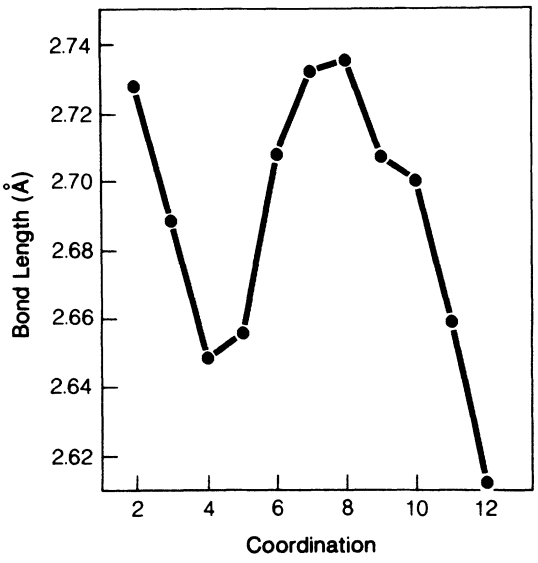

FIG. 10. Bond length as a function of coordination for Si_n. Note the minima at coordination numbers corresponding to the covalent case (a CN of 4) and the metallic case (a CN of 12).

bors are formed, but not for a CN of 8. The decrease in bond length from a CN of 2 to 4 is not expected from quantum-mechanical calculations and is probably a failing of our potential.

In Fig. 11, we present the bond-angle distribution. While previous potentials based on $\cos\theta$ were often designed to favor tetrahedral angles θ_t [as though an energy term proportional to $(\cos\theta-\cos\theta_t)^2$], there is no such bias in our potential. We find that the bond angles are all concentrated near $\theta=\pi/3$ (close packing) or near θ_t (tetrahedral packing). Given our $\cos(3\theta)$ functional form, we might have expected this behavior. However, the virtual absence of bond angles near $\pi/2$ reflects certain geometrical constraints which one might not have anticipated. These packing constraints in effect amplify the significance of the "covalent-metallic" distinction.

Unlike the case of crystalline silicon, the experimental and theoretical "data base" for clusters is quite sparse. For crystalline silicon we have structural information from rather complete pressure work, both experiment and theory, as evidenced in Figs. 1 and 2, and Tables II and III. For clusters we must rely on more indirect comparisons to verify the predictions of the cluster model.

Some recent experimental data do seem to support our predictions. The size dependence of the rate constant[31] for the addition of the first C_2H_4 molecule on to S_n^+ is shown in Fig. 12. For $n \leq 12$ the rate constant k_2 is an erratic function of n, as expected from the variety of cluster geometries calculated for $n \leq 10$ by quantum-chemistry methods.[2] For $n \geq 13$ and $n \geq 19$ smooth rises in k_2 are observed. We interpret this behavior as indicative of a common core with a repeated building block, i.e., a geometric growth sequence. We suggest that the nonreactive minima at $n=13$, 19, and 23 correspond to our icosahedral structures. We expect that uncapped or completely capped icosahedra containing only sixfold-coordinated atoms have minimal reactivities, whereas the C_2H_4 molecules will react when there are at least two nearest-neighbor fourfold-coordinated adatoms. Denoting these adatoms by Si*, the reactive configuration could be the bridge Si*—H—CH=CH—H—Si*. If so, then the C_2H_4 reactivity with one Si* adatom is little more than that with none. In Fig. 13, we illustrate the capping process for $n=13$, 14, and 15.

Our results indicate that in the range of $10 \leq n \leq 20$, the Si_n cluster structures oscillate between metallic pentagonal growth structures and covalent molecular structures. In effect, in this range Si_n clusters border on a

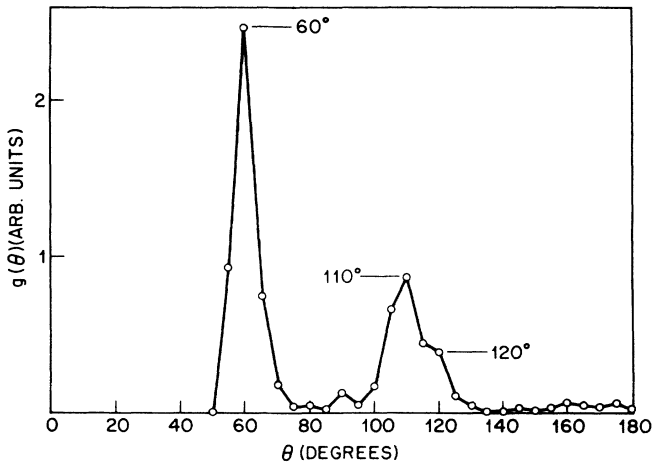

FIG. 11. Angular distribution function for Si_n averaged over $n \leq 20$. Note that almost all the bond angles lie either at the metallic ($\theta=60°$) or covalent ($\theta=109.5°$) limits.

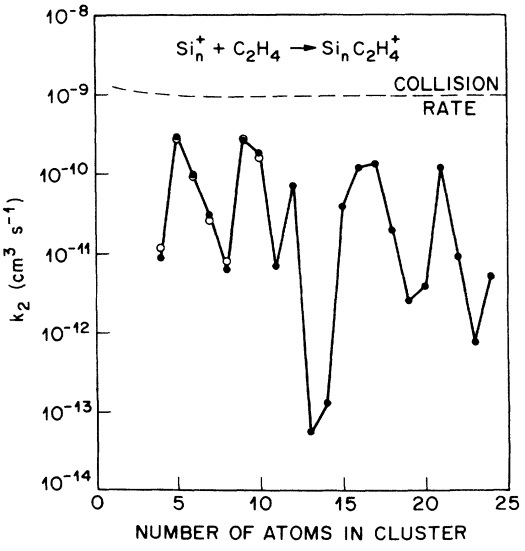

FIG. 12. Rate constants for the addition of the first C_2H_4 to Si_n^+ as measured by Jarrold *et al.* (Ref. 31).

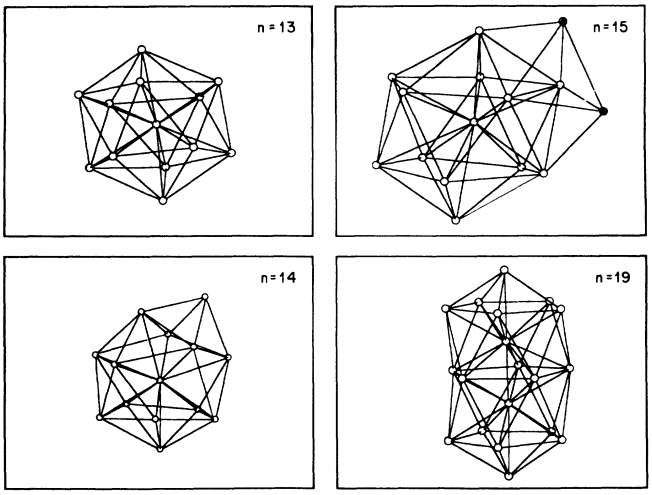

FIG. 13. Pentagonal growth clusters for Si_n as obtained from our interatomic force field for $n=13-15$, 19. For $n=15$ the atoms denoted by Si* in the text are shaded.

"covalent-metallic" phase transition. It may well be that in the addition reaction, the covalent molecule C_2H_4 remains intact and reacts strongly only with fully covalent Si_n structures, such as $n=10$ and 16, and much more weakly with metallic structures, such as $n=13$ and 19. Until first-principles calculations of medium-size clusters become available, it is difficult to say how accurate our model is in calculating small energy differences between covalent and metallic structures for a given n. However, we have varied the magnitude of our backbonding term by as much as factor of 2, i.e., we have changed μ from 4 to 2, and find that our qualitative conclusions remain unchanged. While our model may not yet address such small energy changes, we feel it has achieved the goal expected for a classical model: it has generated plausible candidate structures suitable for first-principle calculations.

IV. CONCLUSIONS

We have presented in detail a new interatomic force field which describes accurately both the phase stability of crystalline silicon, as well as the structures of small and medium-size clusters of silicon. Our force field differs from previous work in two fundamental aspects. First, we show that when three-body forces are adjusted to describe a "covalent→metallic" phase transition instead of small amplitude atomic vibrations, a simple and accurate force field is obtained. As the bond angle θ changes from metallic ($\theta=\pi/3$) to covalent ($\theta=2\pi/3$), we expect to see a rapid transition in the bond character. Thus, our force field is based on an angular function which behaves as $\cos(3\theta)$, as opposed to $\cos(\theta)$. Using this form of the potential we are able to generate for the first time equations of state for crystalline silicon which achieve an accuracy comparable to that obtained from quantum-mechanical calculations. For example, we are able to predict the diamond-to-white-tin transition pressure to within $\sim 20-30\%$.

The second aspect of our work which differs from previous efforts is the explicit inclusion of a term which transfers bond strength from dangling bonds to back bonds. With this term our bulk interatomic force field is simply modified to obtain energies and structures of Si_n vapor-phase clusters. Small silicon clusters would have open polycyclic structures without this backbonding term. From highly accurate molecular orbital calculations, we know small silicon clusters actually assume close-packed, or metalliclike, structures. Our backbonding force is able to reproduce accurately the coordination trends obtained from the quantum-chemistry work. Moreover, we predict surprising pentagonal growth structures for clusters in the range $n=13-25$. These structures partially explain magic numbers recently observed in the addition reaction of C_2H_4 with Si_n^+.

We believe that the success of our interatomic force field for silicon for a wide variety of bonding configurations bodes well for widespread applications. For example, one might use such a force field to study the formation and activation energies for diffusion of intrinsic defects in crystalline silicon, or perhaps the structural properties of amorphous and liquid silicon. This is the first time a classical force field has been successful in describing the condensed properties of any element which is not an inert gas.

ACKNOWLEDGMENTS

One of us (J.R.C.) would like to acknowledge support for this work by the Division of Materials Research, Office of Basic Energy Sciences, U.S. Department of Energy, under Grant No. DE-FG02-89ER45391 and by the Minnesota Supercomputer Institute, and to express his appreciation to AT&T Bell Laboratories for its hospitality.

[1]M. T. Yin and M. L. Cohen, Phys. Rev. B **26**, 5668 (1982).
[2]K. Raghavachari, J. Chem. Phys. **83**, 3520 (1985); **84**, 5672 (1986); K. Raghavachari and C. M. Rohlfing, *ibid.* **89**, 2219 (1988).
[3]Y. Liu, Q.-L. Zhang, F. K. Tittel, and R. E. Smalley, J. Chem. Phys. **85**, 7434 (1986); J. C. Phillips, *ibid.* **89**, 2090 (1988).
[4]F. Stillinger and T. Weber, Phys. Rev. B **31**, 5262 (1985).
[5]R. Biswas and D. R. Hamann, Phys. Rev. Lett. **55**, 2001 (1985); Phys. Rev. B **36**, 6434 (1987).
[6]J. Tersoff, Phys. Rev. Lett. **56**, 632 (1986).
[7]B. W. Dodson, Phys. Rev. B **35**, 2795 (1987).
[8]M. I. Baskes, Phys. Rev. Lett. **59**, 2666 (1987).
[9]E. Blaisten-Barojas and D. Levesque, Phys. Rev. B **34**, 3910 (1986).
[10]B. Feuston, R. K. Kalia, and P. Vashista, Phys. Rev. B **37**, 6297 (1988).
[11]S. Saito, S. Ohnishi, and S. Sugano, Phys. Rev. B **33**, 7036 (1986).
[12]C. H. Patterson and R. P. Messmer (unpublished).
[13]J. R. Chelikowsky, J. C. Phillips, M. Kamal, and M. Strauss,

Phys. Rev. Lett. **62**, 292 (1988); J. R. Chelikowsky and J. C. Phillips, *ibid.* **63**, 1653 (1989).
[14]F. D. Murnaghan, Proc. Nat. Acad. Sci. USA **3**, 244 (1944).
[15]K. J. Chang and M. L. Cohen, Phys. Rev. B **31**, 7819 (1985).
[16]J. Z. Hu, L. D. Merkle, C. S. Menoni, and I. L. Spain, Phys. Rev. B **34**, 4679 (1986).
[17]J. Jamieson, Science **139**, 762 (1963).
[18]G. J. Piermarini and S. Block, Rev. Sci. Instrum. **46**, 973 (1975); W. A. Weinstein and G. J. Piermarini, Phys. Rev. B **12**, 1172 (1975).
[19]H. Olijnyk, S. K. Sikka, and W. B. Holzapfel, Phys. Lett. **103A**, 137 (1974).
[20]J. Z. Hu and I. L. Spain, Solid State Commun. **51**, 263 (1984).
[21]P. Ballone, W. Andreoni, R. Car, and M. Parrinello, Phys. Rev. Lett. **60**, 271 (1988); D. Tomanek and M. Schluter, *ibid.* **56**, 1055 (1986); Phys. Rev. B **36**, 1208 (1987).
[22]P. C. Kelires and J. Tersoff, Phys. Rev. Lett. **61**, 562 (1988).
[23]J. C. Tully, G. M. Gilmer, and M. Shugard, J. Chem. Phys. **71**, 1630 (1979); R. Biswas and D. R. Hamann, Phys. Rev. B **34**, 895 (1986).
[24]C. S. Wang and J. L. Chen (unpublished).
[25]M. R. Hoare and P. Pal, Adv. Phys. **20**, 161 (1971).
[26]O. Echt, K. Sattler, and E. Recknagel, Phys. Rev. Lett. **47**, 1121 (1981).
[27]H. C. Andersen (private communication).
[28]The parameters (a,b) are $a=0.001$ and $b=1.431$ with $E_b=4.90$. We do not associate great physical significance to these parameters. We have applied a macroscopic model to microscopic clusters.
[29]M. F. Jarrold and J. E. Bower (unpublished).
[30]D. J. Trevor, D. M. Cox, K. C. Reichmann, R. O. Brickman, and A. Kaldor, J. Inorg. Chem. **91**, 2598 (1987).
[31]M. F. Jarrold, J. E. Bower, and K. Creegan, J. Chem. Phys. **90**, 3615 (1989).